Available online at https://link.springer.com/journal/42241
http://www.jhydrodynamics.com
Journal of Hydrodynamics, 2022, 34(1): 76-84
https://doi.org/10.1007/s42241-022-0008-5

Numerical simulations of sloshing waves in vertically excited square tank by improved MPS method

Guan-yu Zhang, Wei-wen Zhao, De-cheng Wan*
Computational Marine Hydrodynamics Lab (CMHL), School of Naval Architecture, Ocean and Civil Engineering, Shanghai Jiao Tong University, Shanghai 200240, China

(Received November 22, 2021, Revised January 23, 2022, Accepted January 24, 2022, Published online February 25, 2022)

Abstract: Faraday wave is a phenomenon of sloshing due to a heave motion of a partially filled tank, which is also called parametric instability or parametric resonance. In the present paper, the phenomenon of faraday wave in a pure heave excited square tank is numerically simulated through the moving particle semi-implicit (MPS) method. The surface tension effect and a new Dirichlet boundary condition for the pressure Poisson equation are considered to avert unphysical fragmentation and clustering of particles in splash simulation. In the numerical simulation, the evolution of wave motion, and the non-linearity together with breaking phenomenon of faraday wave can be observed. The agreement is good in general, both amplitude and phase. Besides, the parameter studies including the excitation frequency and the forcing amplitude are carried out to analyses the mechanism of resonances response.

Key words: Liquid sloshing, faraday wave, moving particle semi-implicit (MPS) method, surface tension, MLParticle-SJTU solver

Introduction

Faraday wave is a phenomenon of sloshing due to a heave motion of a partially filled tank. This kind of free surface flow phenomena are quite common, such as VLCC, LNG or huge tank under seismic wave, road transport vehicle, the liquid fuels in spacecraft, which can also be called parametric instability or parametric resonance. In some extreme circumstances, Faraday wave may have violently nonlinear behaviour, even breaking, which may cause devastating damage. Therefore, it is of great importance for researchers and designers to understand the trigger conditions of Faraday waves and the mechanism of the nonlinear and breaking phenomenon.

Sloshing waves in vertically excited tanks have been studied theoretically, experimentally, and numerically in the past several decades and many significant phenomena have been considered in those studies. The first available investigation was performed by Faraday[1] who focused on studying the free surface behaviour as a function of vertical tank motion. Benjamin and Ursell[2] found that the governing equation of Faraday wave could be expressed as the Mathieu equation. Frandsen[3] obtained a numerical solution of the parametric sloshing by the perturbation method. Frandsen and Peng[4] conducted experiments to investigate the sloshing waves in square tanks, and a breaking-mushroom wave was found in vertically excited tanks. Zhuang and Wan[5] used the naoe-FOAM-SJTU solver based on finite volume method (FVM) to simulate the FPSO motion coupled with LNG sloshing. Jin et al.[6] experimentally and numerically conducted the investigation of nonlinear Faraday waves. Liu et al.[7] simulated two-layered liquid sloshing through numerical model NEWTANK established on spatially averaged Navier-Stokes equations.

To simulate this type of sloshing phenomenon, a particle-based method is used in this work, based on the moving particle semi-implicit (MPS) method developed by Koshizuka and Oka[8]. Since particle methods have excellent advantages in dealing with the large deformation and strong nonlinear phenomenon of free surfaces, as well as the moving boundaries, numerous good works employing MPS method are carried out to study violent free surface flow, for instance, dam-break flow[9-10], water entry problems[11], the liquid sloshing problems[12-13], wave-ship interac-

Project supported by the National Natural Science Foundation of China (Grant Nos. 52131102, 51909160 and 51879159), the National Key Research and Development Program of China (Grant No. 2019YFB1704200).
Biography: Guan-yu Zhang (1994-), Female, Ph. D.,
E-mail: yugagaga@sina.com
Corresponding author: De-cheng Wan,
E-mail: dcwan@sjtu.edu.cn

tion[14], multiphase flow[15-17], fluid-structure interaction[18-22] and so on.

In this study, some improvements based on MPS method are proposed for the liquid sloshing simulation, including the surface tension in Navier-Stokes equations and a new Dirichlet boundary condition for the pressure Poisson equation. The continuum surface force (CSF) model developed by Brackbill et al.[23] is used in this paper to consider the surface tension effect at the surface in single-phase flow. Alam et al.[24] simulated the water splash phenomena of high-speed vessels based on MPS method with and without surface tension, and it concluded that the surface tension have a strong effect on splash phenomena. Khayyer et al.[25] proposed a novel surface tension model for simulating the water drop phenomenon, which can avoid the unphysical fragmentation. In addition, various works have focused on the treatment of free surface particles in solving pressure Poisson equation (PPE), such as Chen et al.[26], Shibata et al.[27] and Zhu et al.[28], the concept of virtual particles is introduced, which is referred to in this paper.

In this work, improved MPS method is applied to simulate the Faraday wave in heave excited tanks and give the investigation of nonlinear free surface behaviour, three dimensionality and wave breaking mechanisms. Firstly, a series of sloshing simulations are carried out to validate the reliability of present method. Then, the parameter studies including the excitation frequency and the forcing amplitude are carried out.

1. MPS method

In this study, MPS method is adopted to investigate the liquid sloshing phenomenon. The theories for the MPS have been presented with details in our previous papers[9-13, 15-19], which will be introduced briefly in this section. Then, the consideration of surface tension and improved Dirichlet boundary conditions in PPE will be detailed described in this section.

1.1 *Governing equations*

The governing equations including continuity equation and momentum equation for viscous incompressible fluid are expressed in Lagrangian form as following:

$$\nabla \cdot \boldsymbol{V} = 0 \tag{1}$$

$$\frac{\mathrm{D}\boldsymbol{V}}{\mathrm{D}t} = -\frac{1}{\rho}\nabla p + \nu \nabla^2 \boldsymbol{V} + \boldsymbol{g} \tag{2}$$

where $\boldsymbol{V}$, ρ, p, ν and $\boldsymbol{g}$ denote the velocity vector, the fluid density, the pressure, the kinematic viscosity and the gravitational acceleration, respectively.

1.2 *Kernel function*

In MPS method, governing equations should be expressed by the particle interaction models based on the kernel function. In order to avoid non-physical pressure oscillation, the kernel function presented by Zhang et al.[12] is employed here:

$$W(r) = \frac{r_e}{0.85r + 0.15r_e} - 1, \quad 0 \le r < r_e \tag{3a}$$

$$W(r) = 0, \quad r_e \le r \tag{3b}$$

where $r = |r_j - r_i|$ is the distance between particle i and j, r_e denotes the influence radius of the target particle. Generally, the radius for particle number density and the gradient model is $r_e = 2.1l_0$ and it is $r_e = 4.01l_0$ for the Laplacian model, where l_0 is the initial particle space.

1.3 *Particle interaction models*

Models of particle interaction include gradient model, divergence model and Laplacian model. These models can be written as:

$$\langle \nabla \phi \rangle_i = \frac{D}{n^0} \sum_{j \ne i} \frac{\phi_j + \phi_i}{|\boldsymbol{r}_j - \boldsymbol{r}_i|^2} (\boldsymbol{r}_j - \boldsymbol{r}_i) \cdot W(|\boldsymbol{r}_j - \boldsymbol{r}_i|) \tag{4}$$

$$\langle \nabla \cdot \boldsymbol{\Phi} \rangle_i = \frac{D}{n^0} \sum_{j \ne i} \frac{(\boldsymbol{\Phi}_j - \boldsymbol{\Phi}_i) \cdot (\boldsymbol{r}_j - \boldsymbol{r}_i)}{|\boldsymbol{r}_j - \boldsymbol{r}_i|^2} W(|\boldsymbol{r}_j - \boldsymbol{r}_i|) \tag{5}$$

$$\langle \nabla^2 \phi \rangle_i = \frac{2D}{n^0 \lambda} \sum_{j \ne i} (\phi_j - \phi_i) \cdot W(|\boldsymbol{r}_j - \boldsymbol{r}_i|) \tag{6}$$

$$\lambda = \frac{\sum_{j \ne i} W(|\boldsymbol{r}_j - \boldsymbol{r}_i|)\, |\boldsymbol{r}_j - \boldsymbol{r}_i|^2}{\sum_{j \ne i} W(|\boldsymbol{r}_j - \boldsymbol{r}_i|)} \tag{7}$$

where ϕ is an arbitrary scalar function, $\boldsymbol{\Phi}$ is an arbitrary vector, D is the number of space dimensions, $\boldsymbol{r}$ is the position vector, λ is a parameter to compensate the errors resulting from the limited range of the kernel function and n^0 is the initial density of the particle number.

1.4 *Pressure Poisson equation*

In MPS method, the pressure of particle is implicitly obtained through solving PPE. In the present paper, the mixed source term method is adopted, which is proposed by Tanaka and Masunaga[29], Lee et al.[30]. Thereby, the incompressible condition is represented by two parts, the particle number density and the divergence of velocity, which can be expressed as follows

$$\left\langle \nabla^2 p^{k+1} \right\rangle_i = (1-\gamma)\frac{\rho}{\Delta t}\nabla \cdot V_i^* - \gamma \frac{\rho}{\Delta t^2}\frac{\left\langle n^k \right\rangle_i - n^0}{n^0} \tag{8}$$

where γ is the weight of the particle number density term between 0 to 1. In this paper, $\gamma = 0.01$ is adopted for all numerical experiments. n^* is the temporal particle density defined as

$$\langle n \rangle_i = \sum_{j \neq i} W\left(\left|\boldsymbol{r}_j - \boldsymbol{r}_i\right|\right) \tag{9}$$

1.5 *Free surface detection*

The detection of free surface particle is of importance in computational accuracy and stability. In this paper, a modified surface particle detection method based on the particle number density and the asymmetry arrangement of neighboring particles is applied, which reference to the thought in Khayyer et al.[31], the detection criterion of free surface particle is shown as:

Particle i is

$$\text{surface particle, if } \left(\frac{\langle n \rangle_i^*}{n^0}\right) < 0.8 \tag{10a}$$

$$\text{inconclusive, if } 0.8 < \left(\frac{\langle n \rangle_i^*}{n^0}\right) < 0.97 \tag{10b}$$

$$\text{internal particle, if } \left(\frac{\langle n \rangle_i^*}{n^0}\right) > 0.97 \tag{10c}$$

$$\langle \boldsymbol{F} \rangle_i = \frac{D}{n^0}\sum_{j \neq i}\frac{(\boldsymbol{r}_i - \boldsymbol{r}_j)}{\left|\boldsymbol{r}_i - \boldsymbol{r}_j\right|} W\left(\left|\boldsymbol{r}_i - \boldsymbol{r}_j\right|\right) \tag{11}$$

where $\boldsymbol{F}$ is a vector which represents the asymmetry distribution of neighboring particles. When the value of $\langle n \rangle_i^* / n^0$ is between 0.80, 0.97, Eq. (10) is used to judge free surface particles. When the particle i satisfying $\langle |\boldsymbol{F}| \rangle_i > \alpha |\boldsymbol{F}|^0$ will be considered as a free surface particle, where α is a parameter with a value of 0.9 in this paper.

1.6 *Boundary condition*

In the present MPS method, the solid boundary is represented by one layer of wall particles and two layers of ghost particles, where the arrangement of ghost particles is to fulfil the particle number density so that the particle interaction can be properly calculated near the solid boundary. The calculation of pressure on wall particles is the same as that of fluid particles, solving by PPE. Whereas the pressures of ghost particles are obtained by interpolation. The advantage of present arrangement is that it can ensure a smooth and accurate pressure field around the solid surface and prevent fluid particles from penetrating into the impermeable boundary.

1.7 *Improved Dirichlet boundary conditions in PPE*

In the original MPS method, the Dirichlet boundary conditions are applied directly to free surface particles. By this means, the pressures of free surface particles are equal to zero. Therefore, the particle interactions between free surface particles do not work, and free surface particles may lead to unphysical fragmentation and clustering in splash phenomena. To overcome this problem, an improved Dirichlet boundary condition is applied in solving PPE. To full fill the particle number density of free surface particles, virtual particles are set over the free surface, as shown in Fig. 1, then the particle number density and pressure Laplacian model (the left-hand side of PPE) of free surface particle i can be expressed as:

$$\langle n \rangle_i = \sum_{j \neq i} W_{ji} + \sum_{\text{virtual}} W_{\text{virtual},i} = n_i^* + \sum_{\text{virtual}} W_{\text{virtual},i} \tag{12}$$

$$\left\langle \nabla^2 p^{k+1} \right\rangle_i = \frac{2D}{n^0 \lambda}\sum_{j \neq i}(p_j - p_i)W_{ji} + \frac{2D}{n^0 \lambda}\sum_{\text{virtual}}(p_{\text{virtual}} - p_i)W_{\text{virtual},i} \tag{13}$$

where n_i^* and $\sum_{\text{virtual}} W_{\text{virtual},i}$ denote the particle number density of actual neighboring particles and virtual neighboring particles around particle i. After introducing the virtual particles, the particle number density $\langle n \rangle_i$ of free surface particle can be regarded as the initial density n^0, the left-hand side of PPE can be written as

$$\left\langle \nabla^2 p^{k+1} \right\rangle_i = \frac{2D}{n^0 \lambda}\sum_{j \neq i}(p_j - p_i)W_{ji} + \frac{2D}{n^0 \lambda}(p_{\text{virtual}} - p_i)(n^0 - n_i^*) \tag{14}$$

where p_{virtual} is the pressure of the virtual particles, which is a constant. The Dirichlet boundary conditions on the virtual particles is applied for the PPE. It should be noted that we do not need to actually locate virtual particles. Therefore, the modified Dirichlet boundary condition does not need increase much of calculation amount.

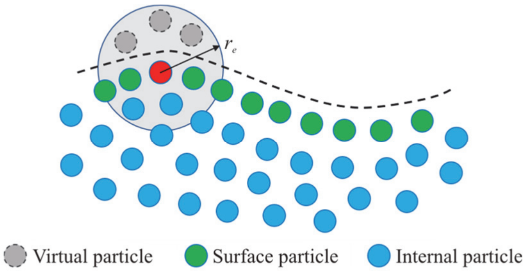

Fig. 1 (Color online) Schematic of free-surface boundary

1.8 *Surface tension in Navier-Stokes equations*

In this paper, the continuous surface force (CSF) model proposed by Brackbill et al.[23] is adopted for simulating the surface tension effect at the interface. The surface tension exerting on the interface is converted into the volume force of fluid around the interface and added to the Navier-Stokes equations, which can be rewritten in the following:

$$\rho \frac{\mathrm{D}\boldsymbol{V}}{\mathrm{D}t} = -\nabla p + \mu \nabla^2 \boldsymbol{V} + \boldsymbol{F}^V + \boldsymbol{F}^S \tag{15}$$

$$\boldsymbol{F}^S = \sigma \kappa \nabla C \tag{16}$$

where $\boldsymbol{F}^S$ represents the volume force component corresponding to the surface tension, σ is the surface tension coefficient, κ is the interface curvature, C is the color function used to mark the particles in different phases, ∇C is the color function gradient. In most existing studies, the color function C is generally defined as:

$$C_i = 1 \quad \text{if} \quad i \quad \text{is the specified phase} \tag{17a}$$

$$C_i = 0 \quad \text{if} \quad i \quad \text{is the other phase} \tag{17b}$$

In this paper, the surface tension only acts on the free surface particles, for the free surface particles $C = 1$, and for the internal particles $C = 0$. In order to ensure the accurate calculation of interface curvature κ, the contoured continuum surface force model (CCSF) proposed by Duan et al.[32] is introduced in this paper. Detailed descriptions of this calculation method are given by Wen et al.[33].

2. Results and discussions

In this section, the wave sloshing in a 3-D heave excited square tank is simulated through the proposed MPS method. In practical application, the Faraday wave generated by vertical excitation has not attracted much attention compared with other sloshing waves. However, in some extreme circumstances, Faraday wave may be violently breaking along with strong loads on the system. Therefore, our main emphasis in this study is to focus on the free surface motion caused by vertical excitation with various excitation frequencies and amplitudes.

The sketch of the 3-D square tank is shown in Fig. 2. The tank size has inner base dimensions of $B \times L = 1\ \mathrm{m}^2 \times 1\ \mathrm{m}^2$, and the water depth is denoted by h, in this paper, $h = 0.2\ \mathrm{m}$. To capture the unaffected motion of free surface, the tank is not equipped with a top cover. The linear sloshing frequencies are defined as:

$$\omega_n = \sqrt{g k_n \tanh(k_n h)} \tag{18}$$

$$k_n = \frac{n\pi}{B} \tag{19}$$

where k_n is the wave number for $n = 0, 1, 2 \cdots, g$ is gravity acceleration. Defining parameter κ_v equals to $a_v \omega_v^2 / g$ as a measure of the importance of vertical forcing. The initial particles spacing (dp) is 0.01 m and the time step is 1×10^{-3} s. The density of fluid is 1 000 kg/m^3. In the simulation, the fluid motion is not initially at rest, a small horizontal excitation is necessary to excite the surface before the tank is moved in a pure vertical motion. In this case, the initial perturbation of 0.0002 m is applied in the first 2 s. The free surface elevation is monitored at the centre of the tank, probe 1 $(x, y) = (B/2, L/2)$.

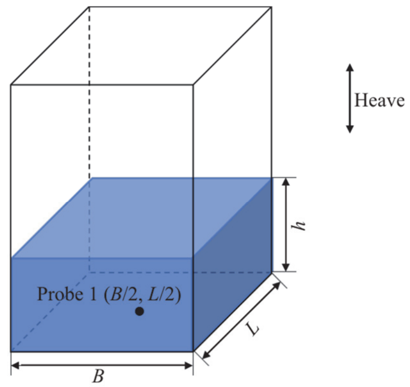

Fig. 2 (Color online) The sketch of the 3-D square tank

2.1 *Numerical validations and discussions*

The accuracy and the reliability of solver are verified in this section. The simulation conditions are the same as those in the experiment of Frandsen and Peng[4]. The excitation frequency and the forcing amplitude are set as $\omega_v = 3.4\omega_1$, $\kappa_v = 0.4$, respectively. Figure 3 displays the wave forms with and without surface tension effect through the present solver, the forms are also compared with the experimental snapshots under the same condition. It can be found that the numerical simulation, both with/without the surface tension effect, can well capture the wave forms at some time instances. Both the "mushroom" type of wave form and the "table-top" wave form with flat crest[34] can be observed. It should also be noted that the fluid splash without the surface tension effect is slightly higher and more apparent than that of considering surface tension and the experimental result. With the surface tension effect, the wave forms obtained by numerical simulation show very good agreement with the experimental results. Therefore, the following simulation should not completely free of surface tension.

In addition, the comparison of time history of free surface motion at Probe 1 between numerical result and experiment data is shown in the Fig. 4, where the excitation frequency and the forcing amplitude are shifted into $\omega_v = 2\omega_1$, $a_v = 0.02\text{ m}$. It can be found that the amplitude of free surface motion increases with time. In general, the numerical results agree well with the experiment, except that the value of wave trough is underestimated by numerical simulation compared with the experiment data. In a word, it can be proved that the present solver is of effectiveness and stableness, either the forms of the excited wave, or the amplitude and phase of the free surface motion are consistent with the experimental result.

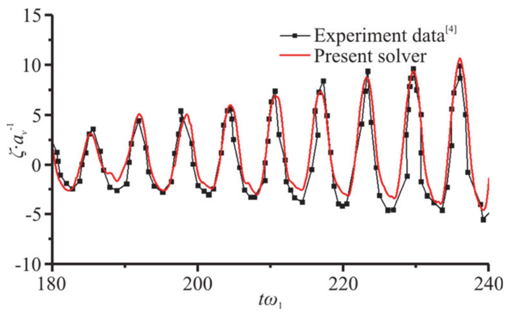

Fig. 4 (Color online) The time history of free surface motion at probe 1

2.2 *parameter study*

In this section, we compared the free surface motion under different forcing amplitudes and excitation frequencies. Firstly, the effects of forcing amplitude on wave forms and free surface motion are analysed. All parameters remain the same, except the forcing amplitude a_v. The excitation frequency is set

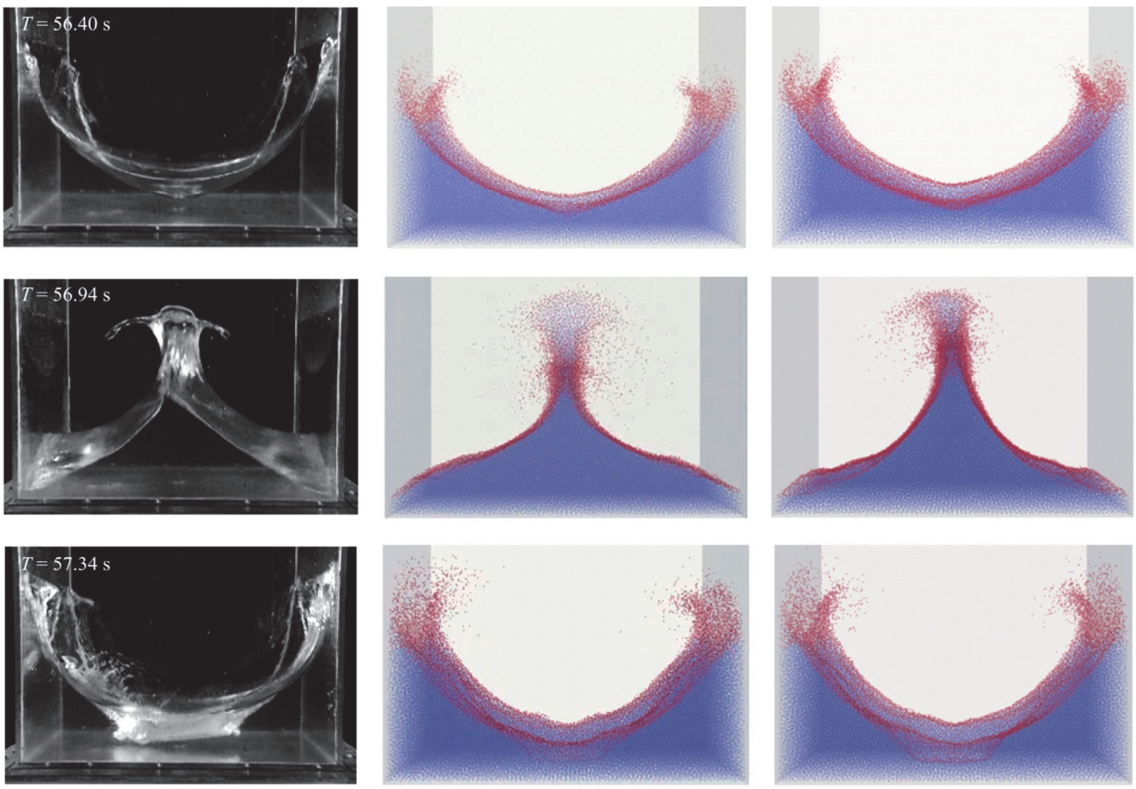

(a) Experimental snapshots (b) Numerical results without the surface tension effect (c) Numerical results with the surface tension effect

Fig. 3 (Color online) The comparison of wave forms between numerical result with/without the surface tension effect and experiment result as $\omega_v = 2\omega_2$, and two forcing amplitudes are applied, $a_v = 0.0250$ m, 0.0045 m, accordingly $\kappa_v = 0.534$, 0.096. Form the Fig. 5, the typical snapshots of wave motion, it can be seen that the problem of surface instability is related to the forcing amplitude. When the forcing amplitude is smaller, as shown in Figs. 5(a_1)-5(a_4), the surface will be quite smooth, but apparent crests can be observed periodically around the middle of the tank with a slightly breaking. When a_v is increased to 0.0250 m as shown in Figs. 5(b_1)-5(b_4), the free surface is rough and irregular, sharp and plunging crests have been formed around the middle of the tank, with fiercely splashing free surfaces and abundant freely falling droplets. In addition,

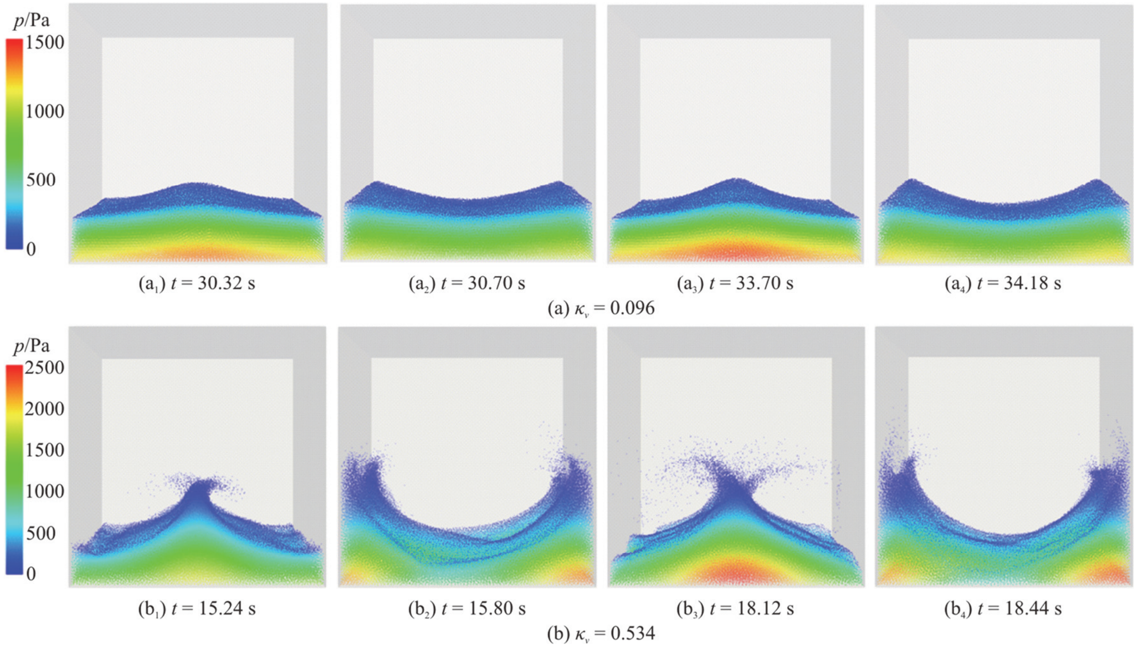

Fig. 5 (Color online) The wave forms under different forcing amplitudes

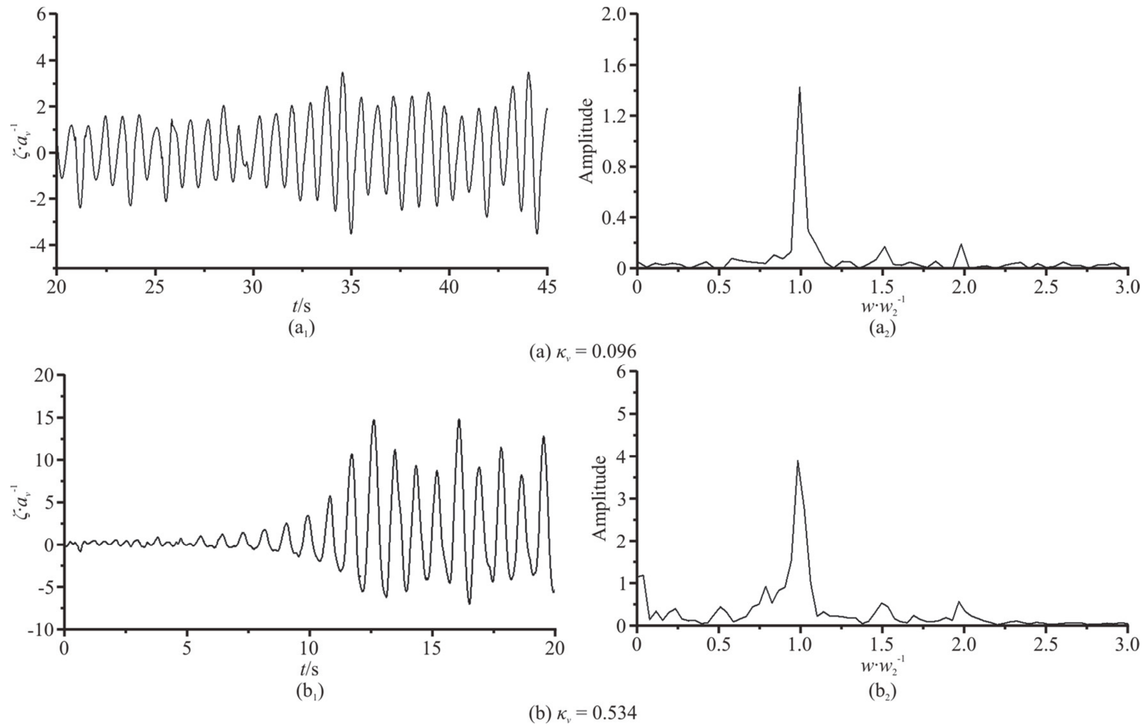

Fig. 6 The time history of the free surface elevation and the FFT result

the interface has apparent 3-D characteristics. The time history of the free surface elevation at probe1 and the fast Fourier transform (FFT) result of surface motion under different forcing amplitudes are shown in Fig. 6. As shown in Figs. 6(a_1), 6(b_1), due to the limitation of water depth, free surface motions always show relatively higher wave peaks, and smaller troughs, which show obvious asymmetric characteristics. When forcing amplitude is relatively smaller, the motion is limited within a certain range and shows slightly randomness. While forcing amplitude is larger, the maximal free surface displacement can reach 10 times of the forcing amplitude, and the motion still shows considerable randomness. For the FFT results, as shown in Figs. 6(a_2), 6(b_2), both two forcing amplitudes are nearly the same, with the dominant and secondary response frequencies being about ω_2, $2\omega_2$, half the forcing frequency and the forcing frequency, respectively.

In addition, the effects of excitation frequency are analysed. Therefore, the excitation frequency ω_v is the only variate. A series of excitation frequencies from $2\omega_1$ to $2\omega_5$ are chosen in this study. The typical snapshots in a period under different excitation frequencies ($\omega_v = 2\omega_1$, $2\omega_2$, $2\omega_3$ and $2\omega_5$) are shown in Fig. 7. It can be seen that when the excitation frequency is close to two times of the nth order natural frequency, the nth modal Faraday wave can be triggered, which means that the number of wave crests and troughs depend on the excitation frequency. Figures 8, 9 illustrate the time histories of free surface motion and the maximum of free surface evolution at the wall under different excitation frequencies. For consistency, the non-dimensional time $t^* w_i$ is used. It can be found that the Faraday wave can be excited only when the excitation frequency is near 2 times the natural frequency.

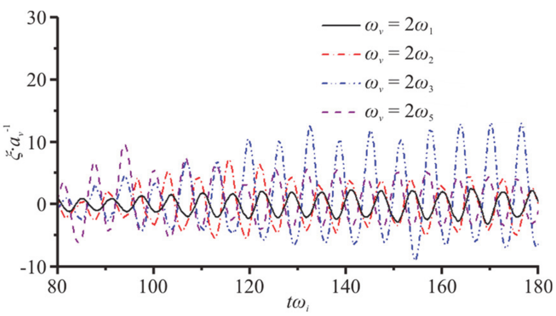

Fig. 8 (Color online) The time history of the free surface elevation under different excitation frequencies

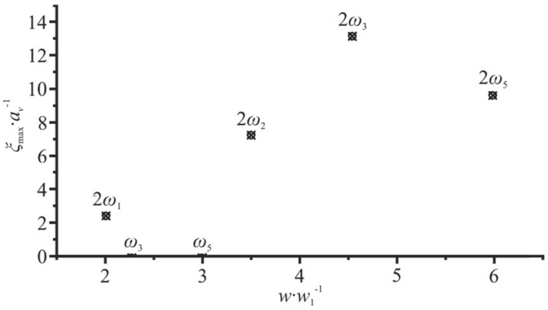

Fig. 9 (Color online) The maximum free surface elevation of different excitation frequencies at the wall

3. Conclusions

In this paper, the MLParticle-SJTU solver based on improved MPS method is employed to investigate the mechanism of Faraday wave in a vertically excited

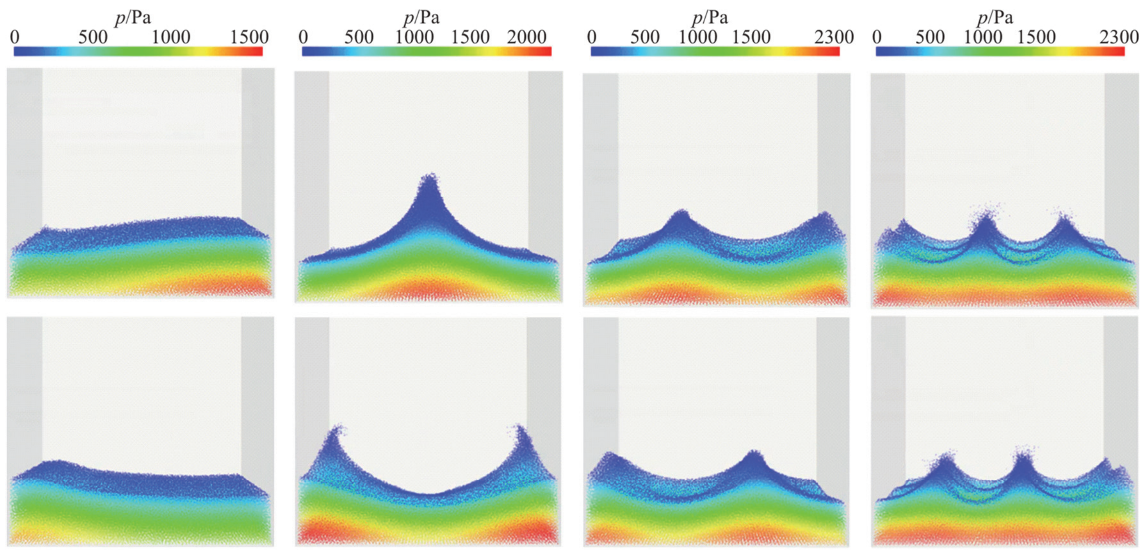

(a) $\omega_v = 2\omega_1$ (b) $\omega_v = 2\omega_2$ (c) $\omega_v = 2\omega_3$ (d) $\omega_v = 2\omega_5$

Fig. 7 (Color online) The wave forms under different excitation frequencies square tank. The surface tension effect and a new Dirichlet boundary condition for PPE are considered to avert unphysical fragmentation and clustering of particles in splash simulation. The numerical results correlate well with experimental data, confirming the reliability of this solver. The fluid splash without the surface tension effect is slightly higher and more apparent than that of considering surface tension and the experimental result. Then, the influences of forcing amplitude and excitation frequency on the formation of Faraday waves are assessed. We have compared the free surface motion under different forcing amplitudes and excitation frequencies. Numerical results show that the surface instabilities depend on the forcing amplitude, the surface instability is more likely when the forced amplitude is increased. In the study of excitation frequency, it can be seen that the nth modal Faraday wave can be triggered when the excitation frequency is close to two times of the nth order natural frequency.

In addition, this paper mainly focuses on free surface motion. However, in some circumstance, it is more important to investigate the impact load caused by Faraday waves. In the future, we will focus on the problem of bang on the bulkhead caused by tank sloshing motion under vertical excitation.

References

[1] Faraday M. On the forms and states assumed by fluids in contact with vibrating elastic surfaces [J]. *Philosophical Transactions*, 1831, 121(52): 319-340.

[2] Benjamin T. B., Ursell F. J. The stability of the plane free surface of a liquid in vertical periodic motion [J]. *Proceedings of the Royal Society of London*, 1954, 225(1163): 505-515.

[3] Frandsen J. B. Sloshing motions in excited tanks [J]. *Journal of Computational Physics*, 2004, 196(1): 53-87.

[4] Frandsen J. B., Peng W. Experimental sloshing studies in sway and heave base excited square tanks [C]. *Sixth International Conference on Civil Engineering in the Oceans*, Baltimore, USA, 2006, 504-512.

[5] Zhuang Y., Wan D. Numerical study on ship motion fully coupled with LNG tank sloshing in CFD Method [J]. *International Journal of Computational Methods*, 2019, 16(6): 1840022.

[6] Jin X., Xue M. A., Lin P. Experimental and numerical study of nonlinear modal characteristics of Faraday waves [J]. *Ocean Engineering*, 2021, 221: 108554.

[7] Liu D., Lin P., Xue M. A. et al. Numerical simulation of two-layered liquid sloshing in tanks under horizontal excitations [J]. *Ocean Engineering*, 2021, 224: 108768.

[8] Koshizuka S., Oka Y. Moving-particle semi-implicit method for fragmentation of incompressible fluid [J]. *Nuclear Science and Engineering*, 1996, 123(3): 421-434.

[9] Tang Z., Zhang Y., Wan D. Multi-resolution MPS method for free surface flows [J]. *International Journal of Computational Methods*, 2016, 13(4): 1641018.

[10] Chen X., Wan D. GPU accelerated MPS method for large-scale 3-D violent free surface flows [J]. *Ocean Engineering*, 2019, 171: 677-694.

[11] Tang Z., Wan D., Chen G. et al. Numerical simulation of 3D violent free-surface flows by multi-resolution MPS method [J]. *Journal of Ocean Engineering and Marine Energy*, 2016, 2(3): 355-364.

[12] Zhang Y. X., Wan D. C., Hino T. Comparative study of MPS method and level-set method for sloshing flows [J]. *Journal of Hydrodynamics*, 2014, 26(4): 577-585.

[13] Xie F. Z., Zhao W. W., Wan D. C. CFD simulations of three-dimensional violent sloshing flows in tanks based on MPS and GPU [J]. *Journal of Hydrodynamics*, 2020, 32(5): 672-683.

[14] Shibata K., Koshizuka S., Sakai M. et al. Lagrangian simulations of ship wave interactions in rough seas [J]. *Ocean Engineering*, 2012, 42: 13-25.

[15] Wen X., Wan D. Numerical simulation of three-layer-liquid sloshing by multiphase MPS method [C]. *Proceedings of the ASME 2018 37th International Conference on Ocean, Offshore and Arctic Engineering, (OMAE2018)*, Madrid, Spain, 2018.

[16] Wen X., Zhao W., Wan D. An improved moving particle semi-implicit method for interfacial flows [J]. *Applied Ocean Research*, 2021, 117: 102963.

[17] Wen X., Zhao W. W., Wan D. C. A multiphase MPS method for bubbly flows with complex interfaces [J]. *Ocean Engineering*, 2021, 238: 109743.

[18] Chen X., Zhang Y., Wan D. Numerical study of 3-D liquid sloshing in an elastic tank by MPS-FEM coupled method [J]. *Journal of Ship Research*, 2019, 63(3): 143-153.

[19] Zhang G., Chen X., Wan D. MPS-FEM coupled method for study of wave-structure interaction [J]. *Journal of Marine Science and Application*, 2019, 18(4): 387-399.

[20] Khayyer A., Gotoh H., Falahaty H. et al. Towards development of a reliable fully-Lagrangian MPS-based FSI solver for simulation of 2D hydroelastic slamming [J]. *Ocean Systems Engineering*, 2017, 7(3): 299-318.

[21] Zhang G., Zhao W., Wan D. Partitioned MPS-FEM method for free-surface flows interacting with deformable structures [J]. *Applied Ocean Research*, 2021, 114: 102775.

[22] Xie F., Zhao W., Wan D. MPS-DEM coupling method for interaction between fluid and thin elastic structures [J]. *Ocean Engineering*, 2021, 236: 109449.

[23] Brackbill J. U., Kothe D. B., Zemach C. A continuum method for modeling surface tension [J]. *Journal of Computational Physics*, 1992, 100(2): 335-354.

[24] Alam A., Kai H., Suzuki K. Two-dimensional numerical simulation of water splash phenomena with and without surface tension [J]. *Journal of Marine Science and Technology*, 2007, 12(2): 59-71.

[25] Khayyer A., Gotoh H., Tsuruta N. A new surface tension model for particle methods with enhanced splash computation [J]. *Journal of Japan Society of Civil Engineers, Ser. B2 (Coastal Engineering)*, 2014, 70(2): 26-30.

[26] Chen X., Xi G., Sun Z. G. Improving stability of MPS method by a computational scheme based on conceptual particles [J]. *Computer Methods in Applied Mechanics and Engineering*, 2014, 278(1): 254-271.

[27] Shibata K., Masaie I., Kondo M. et al. Improved pressure calculation for the moving particle semi-implicit method [J]. *Computational Particle Mechanics*, 2015, 2(1): 91-108.

[28] Zhu Y., Jiang S. Y., Yang X. T. et al. Study on pressure oscillation in particle method [J]. *Chinese Journal of*

Computational Mechanics, 2018, 035(005): 574-581(in Chinese).

[29] Tanaka M., Masunaga T. Stabilization and smoothing of pressure in MPS method by quasi-compressibility [J]. *Journal of Computational Physics*, 2010, 229(11): 4279-4290.

[30] Lee B. H., Park J. C., Kim M. H. et al. Step-by-step improvement of mps method in simulating violent free-surface motions and impact-loads [J]. *Computer Methods in Applied Mechanics and Engineering*, 2011, 200(9-12): 1113-1125.

[31] Khayyer A., Gotoh H., Shao S. D. Enhanced predictions of wave impact pressure by improved incompressible SPH methods [J]. *Applied Ocean Research*. 2009. 31(2): 111-131.

[32] Duan G., Koshizuka S., Chen B. A contoured continuum surface force model for particle methods [J]. *Journal of Computational Physics*, 2015, 298: 280-304.

[33] Wen X., Zhao W. W., Wan D. C. Numerical simulations of multi-layer-liquid sloshing by multiphase MPS method [J]. *Journal of Hydrodynamics*, 2021, 33(5): 938-949.

[34] Lei J., Perlin M., Schultz W. W. Period tripling and energy dissipation of breaking standing waves [J]. *Journal of Fluid Mechanics*, 1998, 369: 273-299.